

Thermostatistics of the polymeric ideal gas

M. A. Gorji* and K. Nozari†

*Department of Physics, Faculty of Basic Sciences,
University of Mazandaran, P.O. Box 47416-95447 Babolsar, Iran*

B. Vakili‡

Department of Physics, Chalous Branch, IAU, P.O. Box 46615-397, Chalous, Iran

In this paper, we formulate statistical mechanics of the polymerized systems in the semiclassical regime. On the corresponding polymeric symplectic manifold, we set up a noncanonical coordinate system in which all of the polymeric effects are summarized in the density of states. Since we show that the polymeric effects only change the number of microstates of a statistical system, working in this coordinate is quite reasonable from the statistical point of view. The results show that the number of microstates decreases due to existence of an upper bound for the momentum of the test particles in the polymer framework. We obtain a corresponding canonical partition function by means of the deformed density of states. By using the partition function, we study thermodynamics of the ideal gas in the polymer framework and show that our results are in good agreement with those that arise from the full quantum consideration at high temperature, and they coincide with their usual counterpart in the limit of low temperature.

PACS numbers: 04.60.Nc, 04.60.Pp, 05.20.-y, 05.30.-d

Key Words: Polymer quantization, Thermodynamics

I. INTRODUCTION

While general relativity (GR) improved our understanding about the Universe, its shortages are revealed when it is utilized to describe dynamics of the Universe in the standard big bang cosmology [1]. With the advent of theories such as inflationary scenarios in order to solve the initial value problem and its later success in explaining the origin of the large scale structures, this idea was formed that classical GR may fail to describe properly our Universe (at least in such high energy regimes) [2]. The fact is that while GR is a classical theory in its original formalism, the quantum effects significantly become important in the very early Universe. It is plausible to expect that the initial value problem will be naturally resolved when a quantum theory of gravity is applied. Although it seems that a complete theory of quantum gravity is not yet made, its main candidates such as string theory and loop quantum gravity revealed some fundamental aspects of the ultimate theory. For example the existence of a minimal measurable length of the order of the Planck length is a common feature of any quantum theory of gravity [3, 4]. Assuming a minimal invariant length, the Heisenberg uncertainty principle trivially implies an ultraviolet cutoff for the system under consideration. However, the standard uncertainty principle cannot support existence of a minimal length and the standard Schrödinger representation of the quantum mechanics is no longer applicable. Therefore, some at-

tempts have been done to include a fundamental length scale in the standard quantum mechanics, see for instance [5] in which the generalized uncertainty principle is introduced with the existence of a minimum measurable length in its formalism. The Hilbert space representation of such modified uncertainty relation is formulated in Ref. [6]. In more recent times, polymer representation of the quantum mechanics has been studied in the context of loop quantum gravity [7]. The associated Hilbert space supports the existence of a minimal length, here known as polymer length scale [8]. The relation between polymer picture and the generalized uncertainty principle framework is investigated in Ref. [9]. A notable character of the polymer representation of quantum mechanics is that, in contrast to the standard Schrödinger representation, in the classical limit $\hbar \rightarrow 0$ the system does not tend to its usual classical version, instead, one recovers a one-parameter λ -dependent classical theory, where $\lambda \sim l_{\text{poly}}/\hbar$ denotes the polymer length scale. The standard classical theory emerges in the continuum limit $\lambda \rightarrow 0$. Exploring the implication of the effective classical λ -dependent theory gives some interesting results. For instance, existence of an upper bound for the energy of a classical systems and removing the big bang singularity in the cosmological setup when it applies to the minisuperspace models [8, 10]. As another feature, we will see that the effective λ -dependent classical theory reproduces some results of the so-called doubly special relativity [11] (in which a minimal observer independent length scale is proposed to special relativity), and polymer length plays the role of the observer independent length scale.

The existence of an invariant minimal length has also interesting effects on the thermodynamical behavior of

* m.gorji@stu.umz.ac.ir

† knozari@umz.ac.ir

‡ b-vakili@iauc.ac.ir

the physical systems. In this regard, many efforts have been made to formulate the statistical mechanics in the framework of the generalized uncertainty principle [12]. Also, thermodynamics of black hole systems in the polymer picture is studied in [13, 14] and the statistical mechanics of the ideal gas in doubly special relativity is investigated in [15]. Nevertheless, in order to study the thermodynamics of a given physical system, one needs to know the microphysics of the system which in turn is determined by quantum mechanics. However, for instance, finding the energy eigenvalues is not an easy task at all when one takes into account the minimal length considerations in the problem at hand [6, 13, 16]. In an alternative picture, one can work with the Hamiltonian and density of states in the corresponding phase space in the semiclassical regime. In this paper, at first we try to formulate the classical phase space of a polymerized systems in terms of the language of the symplectic geometry. Then we formulate statistical mechanics of the polymerized systems in the semiclassical regime. We show that our results are in good agreement with their quantum counterparts.

The structure of the paper is as follows: In section 2, we define a polymeric structure on the symplectic manifold. In section 3, we obtain a deformed density of states that contains all the polymeric effects. Using the deformed density of states, we find a canonical partition function for the polymerized systems. In section 4, we study the polymeric effects on the thermodynamics of the ideal gas through the polymeric partition function. Section 5 is devoted to the conclusions.

II. POLYMERIZATION

In the Hamiltonian formulation of the classical mechanics, the kinematics of the phase space is formed by the Poisson algebra

$$\{q, p\} = 1, \quad (1)$$

where (q, p) are the phase space variables known as canonical variables. Then, quantization is the passage from the classical Poisson algebra (1) to the quantum Heisenberg algebra by the standard rule: Replacing the Poisson bracket by the Dirac commutator for the operators counterpart of the canonical variables as

$$[\hat{q}, \hat{p}] = i\hbar \hat{1}, \quad (2)$$

where \hbar is the Planck constant. It is easy to see that the Heisenberg uncertainty principle is a straightforward result of the commutation relation (2). The ordinary Schrödinger picture of quantum mechanics is based on the representation of operators on the Hilbert space $\mathcal{H} = L^2(\mathbb{R}, dq)$, the space of the square integrable functions with respect to the Lebesgue measure dq on the real line \mathbb{R} . In addition to this well-known representation, there are other representations based on which one can

construct the quantum kinematics. Here, we are going to pursue a case that has been presented in [8] under the name of polymer representation. The polymer representation of quantum mechanics is formulated on the Hilbert space $\mathcal{H}_{\text{poly}} = L^2(\mathbb{R}_d, d\mu_d)$, where $d\mu_d$ is the Haar measure, and \mathbb{R}_d is the real line but now endowed with the discrete topology [17]. The extra structure in polymer picture is properly described by a dimension-full parameter λ such that the standard Schrödinger representation will be recovered in the continuum limit $\lambda \rightarrow 0$ [8]. Evidently, the classical limit of the polymer representation $\hbar \rightarrow 0$, does not yield to the classical theory from which one has started but to an effective λ -dependent classical theory which may be interpreted as a classical discrete theory. Such an effective theory can also be extracted directly from the standard classical theory (without any attribution to the polymer quantum picture) by using the Weyl operator [10]. The process is known as *polymerization* with which we will deal in the rest of this paper.

In polymer representation of quantum mechanics, the position space (with coordinate q) is assumed to be discrete with discreteness parameter λ and consequently the associated momentum operator \hat{p} , that would be a generator of the displacement, does not exist [7]. However, the Weyl exponential operator (shift operator) correspond to the discrete translation along q is well defined and effectively plays the role of momentum for the system under consideration [8]. Taking this fact into account, one can utilize the Weyl operator to find an effective momentum in the semiclassical regime. Therefore, the derivative of the state $f(q)$ with respect to the discrete position q can be approximated by means of the Weyl operator as [10]

$$\begin{aligned} \partial_q f(q) &\approx \frac{1}{2\lambda} [f(q + \lambda) - f(q - \lambda)] \\ &= \frac{1}{2\lambda} \left(\widehat{e^{ip\lambda}} - \widehat{e^{-ip\lambda}} \right) f(q) = \frac{i}{\lambda} \widehat{\sin(\lambda p)} f(q), \end{aligned} \quad (3)$$

and similarly the second derivative approximation gives

$$\begin{aligned} \partial_q^2 f(q) &\approx \frac{1}{\lambda^2} [f(q + \lambda) - 2f(q) + f(q - \lambda)] \\ &= \frac{2}{\lambda^2} (\widehat{\cos(\lambda p)} - 1) f(q). \end{aligned} \quad (4)$$

Inspired by the above approximations, the polymerization process is defined for the finite values of the parameter λ as

$$\hat{p} \rightarrow \frac{1}{\lambda} \widehat{\sin(\lambda p)}, \quad \hat{p}^2 \rightarrow \frac{2}{\lambda^2} (1 - \widehat{\cos(\lambda p)}). \quad (5)$$

The (quantum) polymerization (5) suggests the classical polymer transformation $\mathcal{P}[F]$ of a function $F(q, p)$ on the phase space as [10]

$$\begin{aligned} \mathcal{P}[F(q)] &= F(q), & \mathcal{P}[p] &= \frac{1}{\lambda} \sin(\lambda p), \\ \mathcal{P}[p^2] &= \frac{2}{\lambda^2} (1 - \cos(\lambda p)), \end{aligned} \quad (6)$$

and in a same manner one can find polymer transformation of the higher powers of momentum p . In this sense,

by a classical *polymerized* system, we mean a system that the transformation (6) is applied to its Hamiltonian.

Now, consider a nonrelativistic physical system with standard Hamiltonian

$$H = \frac{p^2}{2m} + U(q), \quad (7)$$

where m is the mass of a particle moving under the act of the potential function $U(q)$. Applying the polymer transformation (6), the associated effective Hamiltonian will be

$$H_\lambda = \frac{1}{m\lambda^2}(1 - \cos(\lambda p)) + U(q). \quad (8)$$

The first consequence of the polymerization (6), which is also clear from the Hamiltonian (8), is that the momentum is periodic and its range should be bounded as $p \in [-\frac{\pi}{\lambda}, +\frac{\pi}{\lambda}]$. In the limit $\lambda \rightarrow 0$, the effective Hamiltonian (8) reduces to the standard one (7) and one recovers the usual range for the canonical momentum $p \in (-\infty, +\infty)$. Therefore, the polymerized momentum is compactified and topology of the momentum sector of the phase space is S^1 rather than the usual \mathbb{R} . As we will see, this structure for the topology of the phase space gives nontrivial results for the polymeric thermodynamical systems, for instance, existence of an upper bound for the internal energy of the system. In order to study the thermodynamics of the polymerized systems, we implement the symplectic geometry which gives a more suitable picture from the statistical point of view.

A. Darboux chart

Consider a two-dimensional symplectic manifold \mathcal{M} thought as a polymeric phase space with symplectic structure ω which is a closed nondegenerate 2-form on \mathcal{M} . According to the Darboux theorem [18], there is always a local chart in which this 2-form takes the canonical form

$$\omega = dq \wedge dp, \quad (9)$$

and as we will see the variables (q, p) may be identified with the canonical variables which we have perviously defined in (1). Although the symplectic structure (9) is canonical in polymeric phase space, one should be careful about the periodic condition for the canonical momentum which significantly leads to the nontrivial topology for the momentum part of the manifold \mathcal{M} . Time evolution of the system is given by the Hamiltonian vector field \mathbf{x}_H which satisfies the equation

$$i_{\mathbf{x}} \omega = dH_\lambda, \quad (10)$$

where H_λ is given by relation (8). By solving the above equation with the use of the effective polymeric Hamiltonian given in (8), one gets

$$\mathbf{x}_H = \frac{\sin(\lambda p)}{m\lambda} \frac{\partial}{\partial q} - \frac{\partial U}{\partial q} \frac{\partial}{\partial p}. \quad (11)$$

The integral curves of the Hamiltonian vector field (11) are the polymer-modified Hamiltonian equations of motion in canonical chart

$$\frac{dq}{dt} = \frac{\sin(\lambda p)}{m\lambda}, \quad \frac{dp}{dt} = -\frac{\partial U}{\partial q}, \quad (12)$$

which clearly reduce to the standard Hamilton's equations in the continuum limit $\lambda \rightarrow 0$.

The Poisson bracket between two real valued functions F and G on \mathcal{M} is defined as

$$\{F, G\} = \omega(\mathbf{x}_F, \mathbf{x}_G). \quad (13)$$

The closure of the 2-form ensures that the Jacobi identity is satisfied by the resultant Poisson brackets in definition (13). In the Darboux chart, we have $\mathbf{x}_F = \frac{\partial F}{\partial p} \frac{\partial}{\partial q} - \frac{\partial F}{\partial q} \frac{\partial}{\partial p}$, and also the same expression for the function G . Substituting these results together with the canonical structure (9) into the definition (13), gives

$$\{F, G\} = \frac{\partial F}{\partial q} \frac{\partial G}{\partial p} - \frac{\partial F}{\partial p} \frac{\partial G}{\partial q}, \quad (14)$$

which is obviously the standard canonical Poisson bracket between two arbitrary functions F and G . It is clear that with choosing $F(q, p) = q$ and $G(q, p) = p$ we have

$$\{q, p\} = 1, \quad (15)$$

which is nothing but the standard canonical Poisson algebra (1). It is important to note that while the polymeric phase space and the standard classical relation (1) from which we have started, seem to have the same kinematical structure, dynamically they are different thanks to the polymer-modified Hamiltonian equations of motion (12). So, the Poisson algebra is canonical in the Darboux chart, but the effective Hamiltonian (8) contains the polymeric effects which will change the dynamics through the relation (10).

Now, suppose that the system under consideration is a many-particle one for which we are going to apply the above formalism in statistical mechanics point of view. To do this, it is necessary to consider the well-known Liouville theorem which is directly related to the number of accessible microstates of the system. The Liouville volume for a $2D$ -dimensional symplectic manifold is defined as

$$\omega^D = \frac{(-1)^{D(D-1)/2}}{D!} \underbrace{\omega \wedge \dots \wedge \omega}_{D \text{ times}}. \quad (16)$$

As a special case we see that for two-dimensional manifolds, the Liouville volume coincides with the symplectic 2-form. According to the Liouville theorem, the Liouville volume (16) is conserved along the Hamiltonian flow \mathbf{x}_H as

$$\mathcal{L}_{\mathbf{x}} \omega^D = 0, \quad (17)$$

where \mathcal{L}_x denotes the Lie derivative along the Hamiltonian vector field \mathbf{x}_H . This relation can be easily deduced from (10) in which we have also noticed that $d\omega = 0$ due to the Cartan formula as $\mathcal{L}_x\omega = i_x d\omega + di_x\omega = 0$ [19, 20]. So, the Liouville theorem is always satisfied on a symplectic manifold independent of a chart in which the physical system is considered.

If we restrict ourselves to a finite one-dimensional spatial volume L , the total volume of the phase space can be obtained by integrating the Liouville volume as

$$\text{Vol}(\omega^1) = \int \omega^1 = \int_L dq \times \int_{-\frac{\pi}{\lambda}}^{+\frac{\pi}{\lambda}} dp = 2\pi \left(\frac{L}{\lambda} \right). \quad (18)$$

In the standard Hamiltonian formalism of the classical mechanics, the total volume of the phase space (18) diverges even if one confines the physical system to a finite spatial volume. More precisely, the momentum part of the integral of Liouville volume will diverge because there is no any priori restriction on the momentum of the test particles in the standard classical mechanics. However, due to existence of an upper bound for the momenta in the classical polymeric systems the resultant total volume (18) will be naturally finite. In other words, compact topology of the momentum part of the polymeric symplectic manifold implies the finite value for the associated total volume that is circumference of a circle with radius λ^{-1} (see Ref. [19] for more details).

Another point here is that, the spatial sector of the phase space volume L should be quantized with respect to the polymer length $l_{\text{poly}} = \alpha \hbar \lambda$, since the polymer length is the possible minimum length for the polymerized system. Here $\alpha = \mathcal{O}(1)$ is a dimensionless coefficient which should be fixed by the experiments [21]. Therefore, we have $\frac{L}{l_{\text{poly}}} \in \mathbb{N}$. This result in some sense is similar to the result obtained in Ref. [22] in the generalized uncertainty principle framework. By taking this fact into account, relation (18) may be rewritten as

$$\text{Vol}(\omega^1) = nh, \quad (19)$$

where n is a positive integer which counts the number of fundamental cells $\hbar \lambda$ exist in L . This equation shows that the total volume of the phase space is naturally quantized with respect to the Planck constant $h = 2\pi \hbar$. Note that in the semiclassical regime, to obtain a finite number of microstates for a given statistical system, one needs an extra assumption that the volume of the phase space is quantized with respect to the Planck constant. However, as our above analysis shows, this issue automatically emerges in the polymerized phase space. The origin of this result may be sought in the Heisenberg uncertainty principle. In the standard phase space there is no restriction according to which the system fails to have access to any desired length scale even the zero length. However, in the polymer picture the theory is equipped with a maximal momentum correspond to the polymer length (below which no other length can be observed) in the light of the uncertainty principle as $p_{\text{max}} \sim \frac{\hbar}{l_{\text{poly}}} \sim \lambda^{-1}$,

the existence of which is responsible for the quantized volume of the phase space.

B. Noncanonical chart

In order to study the statistical physics of a polymerized systems, we introduce a noncanonical transformation

$$(q, p) \rightarrow (q', p') = \left(q, \frac{2}{\lambda} \sin\left(\frac{\lambda p}{2}\right) \right), \quad (20)$$

on the polymeric phase space which transforms effective Hamiltonian (8) to the nondeformed one: $H_\lambda(q, p) \rightarrow H_\lambda(q', p')$, with

$$H_\lambda(q', p') = \frac{p'^2}{2m} + U(q'). \quad (21)$$

Although Hamiltonian (21) is independent of the parameter λ , the new momentum p' is bounded as $p' \in [-\frac{2}{\lambda}, +\frac{2}{\lambda})$ due to the transformation (20). Therefore, the Hamiltonian (21) should be counted distinct from the standard nondeformed Hamiltonian (7). It is also important to note that while the Hamiltonian gets the standard form, the corresponding 2-form in the noncanonical chart becomes

$$\omega = \frac{dq' \wedge dp'}{\sqrt{1 - (\lambda p'/2)^2}}. \quad (22)$$

Substituting the above symplectic structure and also the associated Hamiltonian (21) into the relation (10), we are led to the following solution for the Hamiltonian vector field

$$\mathbf{x}_H = \sqrt{1 - (\lambda p'/2)^2} \left(\frac{p'}{m} \frac{\partial}{\partial q'} - \frac{\partial U}{\partial q'} \frac{\partial}{\partial p'} \right). \quad (23)$$

The integral curves of the above Hamiltonian vector field are the polymer-modified Hamilton's equation in the non-canonical chart

$$\begin{aligned} \frac{dq'}{dt} &= \frac{p'}{m} \sqrt{1 - (\lambda p'/2)^2}, \\ \frac{dp'}{dt} &= -\frac{\partial U}{\partial q'} \sqrt{1 - (\lambda p'/2)^2}, \end{aligned} \quad (24)$$

which will be reduced to the standard ones in the limit of $\lambda \rightarrow 0$. The two sets of modified Hamiltonian equations of motion (12) and (24) are in agreement with each other through the transformation (20).

The Poisson bracket between two real valued functions F and G in this chart can be obtained by substituting the noncanonical structure (22) and the associated vector field (23) into the definition (13) with the result

$$\{F, G\} = \sqrt{1 - (\lambda p'/2)^2} \left(\frac{\partial F}{\partial q'} \frac{\partial G}{\partial p'} - \frac{\partial F}{\partial p'} \frac{\partial G}{\partial q'} \right). \quad (25)$$

With the help of this relation the Poisson bracket of the noncanonical variables q' and p' can be obtained as

$$\{q', p'\} = \sqrt{1 - (\lambda p'/2)^2}, \quad (26)$$

which reduces to its nondeformed counterpart in the continuum limit $\lambda \rightarrow 0$.

Since, by definition, the total volume is invariant over the symplectic manifold, it should be the same as one in the Darboux chart (18). Indeed, integrating the Liouville volume which is nothing but the 2-form structure for a two-dimensional manifold, gives the total volume in the noncanonical chart as

$$\text{Vol}(\omega^1) = \int_L dq' \times \int_{-\frac{2}{\lambda}}^{+\frac{2}{\lambda}} \frac{dp'}{\sqrt{1 - (\lambda p'/2)^2}} = 2\pi \left(\frac{L}{\lambda}\right), \quad (27)$$

that coincides with relation (18) as expected. Therefore, one can work in two equivalent pictures on the polymeric symplectic manifold: *i*) utilizing the effective Hamiltonian (8) together with the symplectic structure (9) in the Darboux chart which leads to the canonical Poisson algebra (15); *ii*) implementing the noncanonical chart with symplectic structure (22), Hamiltonian function (21) and the corresponding noncanonical Poisson algebra (26). The trajectories on the polymeric phase space are the same in two charts since equation (10) is satisfied in a chart-independent manner. However, as we will see in the next section, working within the noncanonical chart is more admissible from the statistical point of view.

III. DENSITY OF STATES AND PARTITION FUNCTION

Statistical mechanics determines the relation between microphysics and macrophysics. All of the thermodynamical properties of a given physical system can be derived from its partition function which is the summation over all accessible microstates of the system. The canonical partition function for a single particle state is defined as [23]

$$\mathcal{Z}_1 = \sum_{\varepsilon} \exp[-\varepsilon/T], \quad (28)$$

where ε are the single particle energy states which are the solution of the Schrödinger equation in the standard representation of quantum mechanics. In fact, the microstates for the statistical system are completely determined by the quantum physics. In contrast to the standard Schrödinger representation, finding the energy eigenvalues in the polymer representation is not an easy task due to the nonlinearity of the quantum Hamiltonian in this picture [7, 8, 16]. Even if one finds the microstates' energies in the polymer picture, calculating the partition function (28) is somehow a complicated issue [13]. Nevertheless, one may work with the classical Hamiltonian together with the density of states in the semiclassical

regime. The semiclassical and the quantum statistics will be coincided in the high temperature regime. Therefore one should be careful that the semiclassical approximation is only applicable for the polymerized systems with small polymer length scale through the uncertainty principle.

Approximating the summation over the energy eigenvalues in the relation (28) by the integral over the phase space volume yields

$$\sum_{\varepsilon} \rightarrow \frac{\text{Vol}(\omega^3)}{h^3} = \frac{1}{h^3} \int_{\mathcal{M}} \omega^3, \quad (29)$$

where ω^3 is the Liouville volume of the six-dimensional phase space of the single particle which in turn, should be obtained by substituting the associated 2-form structure into the definition (16). Relation (29) is written in a chart-independent manner on the manifold since the total volume $\text{Vol}(\omega^3)$ is invariant over the symplectic manifold (see also [19]). Indeed, equation (29) is nothing but the Heisenberg uncertainty principle which implies a finite fundamental element for the phase space volume of the order of Planck constant. The total volume determines the number of microstates of the system and it, as is guaranteed by the Liouville theorem, should be invariant under the time evolution. Now, one may consider relation (29) in various charts over symplectic manifolds with no worries about the invariance of the total volume as time grows, since the Liouville theorem is satisfied in a chart-independent manner via the relation (17).

In the usual statistical mechanics, the topology of the phase space of a single particle is \mathbb{R}^6 and then relation (29) in the Darboux (canonical) chart leads to the well-known result,

$$\sum_{\varepsilon} \rightarrow \frac{1}{h^3} \int \int \int dx dy dz \times \int_{-\infty}^{+\infty} \int_{-\infty}^{+\infty} \int_{-\infty}^{+\infty} dp_x dp_y dp_z. \quad (30)$$

With approximating the summation over the energy eigenvalues in (28) by relation (30), one can obtain the standard definition of the semiclassical partition function [24]. In the same way, the polymeric partition may be achieved.

We consider (29) for the polymerized phase space in two charts: the Darboux and noncanonical charts which we presented in the previous section. In the Darboux chart, the density of states takes the same form as the usual one (30) because the corresponding symplectic structure (9) is canonical (see the appendix), with this difference that now the momentum part of the polymeric phase space has a compact topology S^1 rather than the usual \mathbb{R} . Thus we have

$$\sum_{\varepsilon} \rightarrow \frac{1}{h^3} \int \int \int dx dy dz \times \int_{-\pi/\lambda}^{+\pi/\lambda} \int_{-\pi/\lambda}^{+\pi/\lambda} \int_{-\pi/\lambda}^{+\pi/\lambda} dp_x dp_y dp_z. \quad (31)$$

Approximating the quantum partition function (28) by the polymeric state density (31) and substituting the as-

sociated Hamiltonian (8) instead of the energy eigenvalues ε , gives the polymeric partition function as

$$\mathcal{Z}_1(\lambda; T, V) = \frac{1}{h^3} \int \int \int \exp \left[-\frac{U(x, y, z)}{T} \right] dx dy dz \times \prod_{i=1}^3 \left(\int_{-\pi/\lambda}^{+\pi/\lambda} \exp \left[-\frac{(1 - \cos(\lambda p_i))}{m\lambda^2 T} \right] dp_i \right). \quad (32)$$

It is clear that both the Hamiltonian and the density of states are modified in the polymer phase space in the Darboux (canonical) chart. Rewriting (29) in the noncanonical chart on the polymeric symplectic manifold, gives the following polymeric density of states in the noncanonical chart (see the appendix)

$$\sum_{\varepsilon} \rightarrow = \frac{1}{h^3} \int \int \int dx' dy' dz' \times \int_{-2/\lambda}^{+2/\lambda} \int_{-2/\lambda}^{+2/\lambda} \int_{-2/\lambda}^{+2/\lambda} \frac{dp'_x dp'_y dp'_z}{\sqrt{\left(1 - \left(\frac{\lambda p'_x}{2}\right)^2\right) \left(1 - \left(\frac{\lambda p'_y}{2}\right)^2\right) \left(1 - \left(\frac{\lambda p'_z}{2}\right)^2\right)}}. \quad (33)$$

Therefore in the noncanonical chart, as the above equation shows, while the Hamiltonian takes the standard form (21) the polymeric effects are summarized in the density of states. Equation (33) determines the number of accessible microstates for the system and because of the bounded domain for the momenta this number is less than when the polymeric effects are absent. A similar result is also achieved in the other effective approaches to quantum gravity such as generalized uncertainty principle [12], doubly special relativity [15] and noncommutative phase space [20]. As a first thermodynamical outcome we can see that the polymeric effects cause a reduction in the entropy of the system. This is because the entropy is directly determined from the number of microstates. In the next section we will explicitly investigate this fact and its following results for a particular case in which the underlying system is a system of an ideal gas.

Following the same steps which led us to (32), but this time with the help of relations (21), (28) and (33), the canonical polymeric partition function for a single noninteracting particle becomes

$$\begin{aligned} \mathcal{Z}_1(T, V) &= \frac{V}{h^3} \prod_{i=1}^3 \left(\int_{-2/\lambda}^{+2/\lambda} \exp \left[-\frac{p_i'^2}{2mT} \right] \frac{dp'_i}{\sqrt{1 - \left(\frac{\lambda p'_i}{2}\right)^2}} \right) \\ &= \frac{V}{h^3 \lambda^3} \left(\exp \left[-\frac{\lambda^{-2}}{mT} \right] I_0 \left[\frac{\lambda^{-2}}{mT} \right] \right)^3, \end{aligned} \quad (34)$$

where V is the result of integration over the spatial part and I_0 denotes the modified Bessel function of the first kind. The expression (34) for the partition function is in an excellent agreement with what is obtained in [13] by the full quantum consideration. Now, the polymeric thermodynamics of a physical system (an ideal gas in our model in the next section) may be extracted by means of the above partition function.

IV. IDEAL GAS

In this section, let us consider a gaseous system consisting of N noninteracting particles at temperature T confined in the volume V . We assume that this system obeys the Maxwell-Boltzmann statistics. Equation (34) can be used to evaluate the corresponding polymeric partition function as

$$\mathcal{Z}_N(T, V) = \frac{1}{N!} [\mathcal{Z}_1(T, V)]^N, \quad (35)$$

in which the Gibb's factor is also considered [24]. The natural choice for the polymer length l_{poly} is the Planck length $l_{\text{poly}} = \alpha \hbar \lambda = \alpha l_{\text{Pl}} = \sqrt{G \hbar}$, where G is the gravitational constant and α is a dimensionless coefficient of the order of unity $\alpha \sim \mathcal{O}(1)$. As we have mentioned before, this coefficient should be fixed only by the experiments [21]. In our study, the value of the coefficient α determines the boundary in which the polymeric effects become important. As we will see, the polymeric effects appear in the trans-Planckian regime for the values $\alpha < 1$ and the sub-Planckian polymeric effects emerge for $\alpha > 1$. Here, we assume $l_{\text{poly}} = l_{\text{Pl}}$, i.e., we select $\alpha = 1$ for the sake of simplicity. Substituting relation (34) into (35) gives the total partition function for the polymerized ideal gas as

$$\mathcal{Z}_N(T, V) = \frac{(V/l_{\text{Pl}}^3)^N}{N!} \left(\exp \left[-\frac{T_{\text{Pl}}^2}{mT} \right] I_0 \left[\frac{T_{\text{Pl}}^2}{mT} \right] \right)^{3N}, \quad (36)$$

where T_{Pl} is the Planck temperature $T_{\text{Pl}} = \sqrt{\frac{\hbar}{G}}$. The prefactor $(V/l_{\text{Pl}}^3) \in \mathbb{N}$ in this equation shows the discreteness of space in the polymer framework. In the following, by means of this expression for the total partition function, we will investigate the thermodynamical properties of the polymeric ideal gas.

A. Pressure

First of all, let us look at the Helmholtz free energy F for the polymeric ideal gas which can be obtained (with the help of (36)) from its standard definition as

$$F = -T \ln [\mathcal{Z}_N(T, V)] \\ = NT \left(\ln \left[\frac{N I_{\text{Pl}}^3}{V I_0^3 [T_{\text{Pl}}^2 / mT]} \right] - 1 \right) + \frac{3NT_{\text{Pl}}^2}{m}, \quad (37)$$

in which we have used the Stirling's approximation $\ln[N!] \approx N \ln[N] - N$ for large N . The pressure by definition is

$$P = - \left(\frac{\partial F}{\partial V} \right)_{T, N} = \frac{NT}{V}. \quad (38)$$

Therefore, the familiar equation of state for the ideal gasses, that is,

$$PV = NT, \quad (39)$$

preserves its form also in the polymer framework.

B. Internal energy

The internal energy of the polymeric ideal gas will be

$$U = -T^2 \left[\frac{\partial}{\partial T} \left(\frac{F}{T} \right) \right]_{N, V} = \frac{3NT_{\text{Pl}}^2}{m} \left(1 - \frac{I_1 [T_{\text{Pl}}^2 / mT]}{I_0 [T_{\text{Pl}}^2 / mT]} \right). \quad (40)$$

This result exactly coincides with what comes from the full quantum consideration of the ideal gas in the polymer picture but now in a simpler manner [13]. It is important to note that we are working in the semiclassical regime while our results are in good agreement with their full quantum counterparts in the limit of high temperature. Therefore, the quantum considerations preserve their importance for the low temperature phenomenons such as Bose-Einstein condensation. Nevertheless, considering the low temperature behavior is useful even in the semiclassical regime to see how the results in this limit may be recovered. To do this, let us take the low temperature limit of the relation (40), that is

$$U \approx U_0 \left(1 + \frac{mT}{4T_{\text{Pl}}^2} \right), \quad (41)$$

where $U_0 = \frac{3}{2}NT$ is the well-known usual internal energy for the ideal gas. A glance at 41) shows that while the polymeric effects becomes important at the high temperatures, the standard relation for the internal energy of an ideal gas is recovered in the limit of low temperature. The usual internal energy (dashed line) and its polymeric counterpart (solid line) versus the temperature are plotted in figure 1. As this figure shows, the two curves coincide at low temperatures and while the temperature rises are separated from each other.

To estimate the order of magnitude of the polymeric correction to the internal energy of an ideal gas, consider

$$\left| \frac{\Delta U}{U} \right| = \left| \frac{U - U_0}{U} \right| \sim \left(\frac{m}{m_{\text{Pl}}} \right) \times \left(\frac{T}{T_{\text{Pl}}} \right), \quad (42)$$

where m_{Pl} is the Planck mass (equal to the Planck temperature in the units in which we are working). Since we have set numerical factor α to be of the order of unity, the polymeric effects become important on the trans-Planckian regime. In this regard, these effects will be very small in the currently accessible temperatures [25]. For instance, consider an ideal gas consisting of electrons with mass $m_e \approx 0.5 \text{ MeV}$. For the temperature about $T \sim 1 \text{ TeV}$ the polymeric correction to the corresponding internal energy is of the order of

$$\left| \frac{\Delta U}{U} \right| \sim 10^{-38}, \quad (43)$$

where we have set $m_{\text{Pl}} \approx 1.2 \times 10^{19} \text{ GeV}$.

Furthermore, the usual internal energy for an ideal gas U_0 is linearly proportional to its temperature and consequently the system can have access to any arbitrary high energy scale just by sufficiently increasing its temperature. However, a glance at the corresponding relation for the polymeric ideal gas given by equation (40) shows the existence of a finite maximum value in the high temperature limit as (see figure 1)

$$U \leq U_{\text{max}} = \frac{3NT_{\text{Pl}}^2}{m}. \quad (44)$$

The fact that no energy scale is accessible greater than the above upper bound may be attributed to fact that the momenta of the noninteracting particles of the gaseous system are bounded in polymer framework.

C. Entropy

Now let us see how the entropy changes its form under the framework we are dealing with. A straightforward calculation based on the Helmholtz energy (37) will arrive us to

$$S = - \left(\frac{\partial F}{\partial T} \right)_{N, V} = N \left(\ln \left[\frac{V I_0^3 [T_{\text{Pl}}^2 / mT]}{N I_{\text{Pl}}^3} \right] + 1 \right) \\ - \frac{3NT_{\text{Pl}}^2}{mT} \frac{I_1 [T_{\text{Pl}}^2 / mT]}{I_0 [T_{\text{Pl}}^2 / mT]}. \quad (45)$$

In figure 2, we have plotted the behavior of entropy in terms of temperature. As this figure shows entropy increases with a much less rate in comparison with the usual ideal gas. This result is due to the fact that entropy is directly related to the number of microstates of the system and this quantity in turn reduces in the polymer framework since there is an upper bound for the momentum of the particles in this picture.

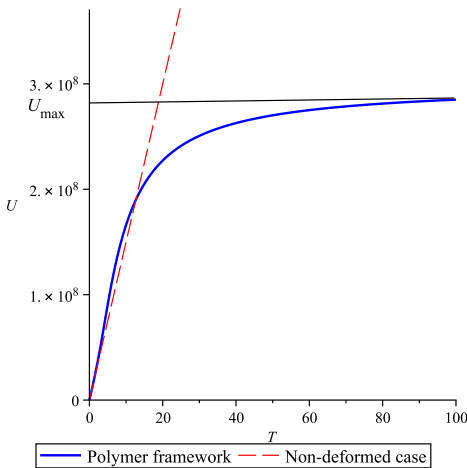


FIG. 1. The internal energy versus the temperature; the solid line represents the internal energy in the polymer framework and the dashed line corresponds to the standard nondeformed case. Clearly, there is an upper bound for the internal energy in the polymer framework which is originated in the existence of the maximal momentum (UV cutoff) in the polymeric systems. The figure is plotted in unit $\hbar = 1$ and $T_{\text{Pl}} = 10$, where T_{P} is the Planck temperature. The number of particles and the mass are taken as $N = 10^7$ and $m = 10$. The polymeric effects dominate when the temperature approaches the Planck temperature.

To see how the entropy behaves in the low temperature regime, we may take this limit of the relation (45) with result

$$S \approx N \left(\ln \left[\frac{V}{N} \left(\frac{2\pi m T}{h^2} \right)^{3/2} \right] + \frac{5}{2} \right) - \frac{3}{4} N \frac{m T}{T_{\text{Pl}}^2}. \quad (46)$$

The last term on the right-hand side is the first order polymeric correction to the entropy of an ideal gas which is negligible in the limit of low temperatures. This is also clear from the figure 2, which shows that the entropy curve (45) coincides with its standard nondeformed one in the limit of low temperature. The order of magnitude of the polymeric correction to the entropy is the same as we obtained for the internal energy.

D. Specific heat

Finally, another important thermodynamical quantity is the specific heat which can be evaluated from the internal energy (40) as follows

$$C_v = \left(\frac{\partial U}{\partial T} \right)_V = \frac{3NT_{\text{Pl}}^4}{m^2 T^2} \left(1 - \frac{mT}{T_{\text{P}}^2} \frac{I_1[T_{\text{Pl}}^2/mT]}{I_0[T_{\text{Pl}}^2/mT]} - \frac{I_1^2[T_{\text{Pl}}^2/mT]}{I_0^2[T_{\text{Pl}}^2/mT]} \right) \quad (47)$$

The specific heat versus the temperature is shown in figure 3. We see that this quantity grows until it reaches

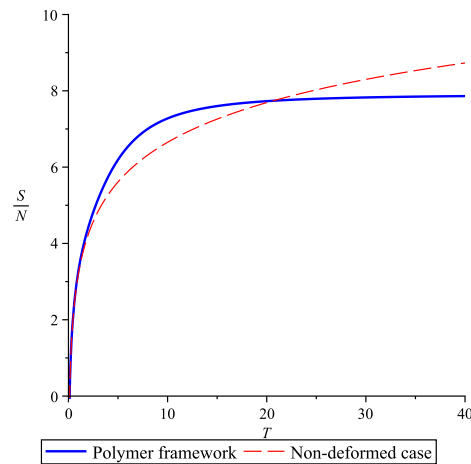


FIG. 2. The entropy against the temperature; the solid line represents the entropy in the polymer picture and the dashed line corresponds to the nondeformed case. The entropy increases with a much less rate in comparison with the ordinary ideal gas since the number of microstates in the polymer picture is less than the usual case. The figure is plotted for $V = 10^7$.

a maximum value and then takes a decreasing behavior, eventually tends to zero. This means that from now on, if the system gets more thermal energy, its internal energy does not change. Such a behavior is expected because we have seen from (44) that the system eventually reaches a saturated internal energy. Again, our result coincides with one arises from the full quantum consideration of the ideal gas for the small polymer length [13].

As we have done in the last two subsections, let us take a look at the low temperature limit of the specific heat, that is

$$C_v \approx \frac{3}{2} N \left(1 + \frac{mT}{2T_{\text{Pl}}^2} \right). \quad (48)$$

Again, it is seen that the polymeric correction is of the order of one that is obtained for the internal energy. Also, as we can see from (48), the specific heat of the polymeric system is coincided with its value for the ordinary ideal gas at very low temperatures.

V. SUMMARY AND CONCLUSIONS

The polymer picture of quantum mechanics is an exotic representation of the commutation relations which have been investigated in a symmetric sector of loop quantum gravity. We argued that in order to study the statistical mechanics of a polymeric systems, analytical evaluation of the energy eigenvalues may be impossible since the Hamiltonian gets a nonlinear form in this framework. On the other hand, we showed one can work with the classical Hamiltonian and the density of states in the semiclassical regime. The advantage of this method is

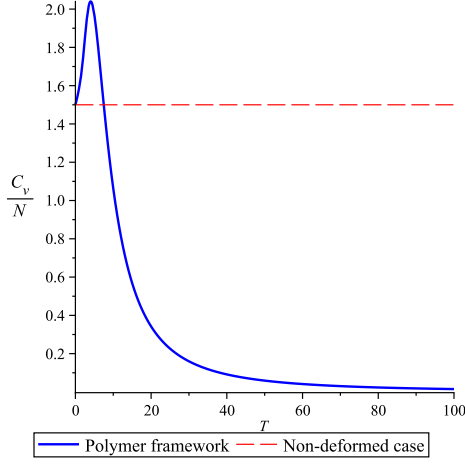


FIG. 3. The specific heat versus the temperature in the polymer framework. Since the increasing behavior of the internal energy stops after reaching to its maximum, it is expected that the specific heat goes to zero after reaching to a maximum value. The figure clearly shows this behavior.

that there is no need to solve the nonlinear eigenvalue problem. Therefore, we considered the symplectic structure of the polymeric phase space and for studying the statistical mechanics in this picture we used the effective Hamiltonian (8) and the deformed density of states (31) in the Darboux chart. Moreover, we introduced a noncanonical chart on the polymeric symplectic manifold in which the Hamiltonian takes the standard form (21) and all the polymeric effects were summarized in the deformed density of states (33). We explained that working in this chart is more admissible from the statistical point of view. This is because the density of states determines the number of accessible microstates of the system and consequently the polymeric effects only change this quantity in this chart. According to our calculations the number of microstates decreased when the polymeric considerations came into the play and we linked this phenomena to the fact that the momenta are bounded in such a framework. Based on the deformed density of states, we obtained the canonical partition function for the polymeric many particle systems and then utilized it to study thermodynamics of the ideal gas. In this regard, some thermodynamical quantities of the polymeric ideal gas such as pressure, internal energy, entropy, and specific heat are evaluated. Having the same form of the equation of state as the ordinary ideal gas, existence of an upper limit for the internal energy unlike the conventional case in which there is no restriction for the system to achieve any level of energy, increasing behavior of the entropy but with a rate much less than the usual case and tending to zero after reaching to a maximum value for the specific heat were the main features of our analysis based on the ideas we have designed in this article. As an estimation, our calculations predict $\sim 10^{-38}$ (in the TeV temperature scale) for the order of magnitude of the polymeric corrections to the thermodynamical quantities of an ideal gas. We saw that these results are in

very good agreement with their counterparts arisen from the full quantum consideration at high temperatures and they coincide with their usual counterparts at the low temperature limit, so this may be considered as evidence that the way we have moved in, was a right way.

Appendix A: Polymeric Density of States

To analyze the thermodynamics of the polymeric ideal gas, we need to consider a six-dimensional phase space corresponding to the single particle state. The homogeneous polymerization for the six-dimensional phase space with variables $q^i = (x, y, z)$ and $p_i = (p_x, p_y, p_z)$ is read from (5) as

$$\begin{aligned} \mathcal{P}[F(q^i)] &= F(q^i), & \mathcal{P}[p_i] &= \frac{1}{\lambda} \sin(\lambda p_i), \\ \mathcal{P}[p_i^2] &= \frac{2}{\lambda^2} (1 - \cos(\lambda p_i)). \end{aligned} \quad (\text{A-1})$$

In the Darboux chart, the canonical structure for the six-dimensional symplectic manifold is

$$\omega = dx \wedge dp_x + dy \wedge dp_y + dz \wedge dp_z, \quad (\text{A-2})$$

where the momenta are bounded as $p_i \in [-\frac{\pi}{\lambda}, +\frac{\pi}{\lambda}]$. The associated 6-form Liouville volume can be obtained by substituting (A-2) into the definition (16) as

$$\omega^3 = dx \wedge dy \wedge dz \wedge dp_x \wedge dp_y \wedge dp_z. \quad (\text{A-3})$$

The density of states corresponding to the structure (A-2) can be obtained via the relation (29) as

$$\sum_{\varepsilon} \rightarrow \frac{1}{h^3} \int d^3 q \times \int_{|p_i| < \frac{\pi}{\lambda}} d^3 p, \quad (\text{A-4})$$

which clearly gives the relation (31). To obtain the state density in the noncanonical chart, we apply transformation (20) to the canonical variables (q^i, p_i) in the polymeric six-dimensional phase space as

$$(q^i, p_i) \rightarrow (q^i, p'_i) = \left(q^i, \frac{2}{\lambda} \sin\left(\frac{\lambda p_i}{2}\right) \right), \quad (\text{A-5})$$

where $q^i = (x', y', z')$ and $p'_i = (p'_x, p'_y, p'_z)$. The 2-form symplectic structure for the six-dimensional symplectic manifold in the noncanonical chart becomes

$$\omega = \frac{dx' \wedge dp'_x}{\sqrt{1 - (\frac{\lambda p'_x}{2})^2}} + \frac{dy' \wedge dp'_y}{\sqrt{1 - (\frac{\lambda p'_y}{2})^2}} + \frac{dz' \wedge dp'_z}{\sqrt{1 - (\frac{\lambda p'_z}{2})^2}}, \quad (\text{A-6})$$

which leads to the 6-form Liouville volume

$$\omega^3 = \frac{dx' \wedge dy' \wedge dz' \wedge dp'_x \wedge dp'_y \wedge dp'_z}{\sqrt{\left(1 - (\frac{\lambda p'_x}{2})^2\right) \left(1 - (\frac{\lambda p'_y}{2})^2\right) \left(1 - (\frac{\lambda p'_z}{2})^2\right)}}, \quad (\text{A-7})$$

through the definition (16). The density of states (33) can be easily deduced by substituting the Liouville volume (A-7) into the relation (29). Relation (33) is essential to obtain the partition function in polymer framework.

-
- [1] W. Rindler, *Gen. Rel. Grav.* **34** (2002) 133
C. B. Collins and S. W. Hawking, *Astrophys. J.* **180** (1973) 317.
- [2] A. H. Guth, *Phys. Rev. D* **23** (1981) 347
A. D. Linde, *Phys. Lett. B* **108** (1982) 389
A. Albrecht and P. J. Steinhardt, *Phys. Rev. Lett.* **48** (1982) 1220.
- [3] D. J. Gross and P. F. Mende, *Nucl. Phys. B* **303** (1988) 407
D. Amati, M. Ciafaloni and G. Veneziano, *Phys. Lett. B* **216** (1989) 41
L. Garay, *Int. J. Mod. Phys. A* **10** (1995) 145.
- [4] C. Rovelli and L. Smolin, *Nucl. Phys. B* **442** (1995) 593
A. Ashtekar and J. Lewandowski, *Class. Quant. Grav.* **14** (1997) A55.
- [5] K. Konishi, G. Paffuti and P. Provero, *Phys. Lett. B* **234** (1990) 276
M. Maggiore, *Phys. Lett. B* **319** (1993) 83
M. Maggiore, *Phys. Rev. D* **49** (1994) 5182.
- [6] A. Kempf, G. Mangano and R. B. Mann, *Phys. Rev. D* **52** (1995) 1108
K. Nozari and A. Etemadi, *Phys. Rev. D* **85** (2012) 104029.
- [7] A. Ashtekar, S. Fairhurst and J. Willis, *Class. Quantum Grav.* **20** (2003) 1031
K. Fredenhagen and F. Reszewski, *Class. Quantum Grav.* **23** (2006) 6577.
- [8] A. Corichi, T. Vukašinac and J. A. Zapata, *Phys. Rev. D* **76** (2007) 044016.
- [9] B. Majumder and S. Sen, *Phys. Lett. B* **717** (2012) 291.
- [10] A. Corichi and T. Vukašinac, *Phys. Rev. D* **86** (2012) 064019.
- [11] G. A. Camelia, *Int. J. Mod. Phys. D* **11** (2002) 35
J. Magueijo and L. Smolin, *Phys. Rev. Lett.* **88** (2002) 190403.
- [12] S. Kalyana Rama, *Phys. Lett. B* **519** (2001) 103
M. Lubo, [arxiv: hep-th/0009162]
M. Lubo, *Phys. Rev. D* **68** (2003) 125004
K. Nozari and B. Fazlpour, *Gen. Rel. Grav.* **38** (2006) 1661
K. Nozari and S. H. Mehdipour, *Chaos Solitons Fractals* **32** (2007) 1637
T. Fityo, *Phys. Lett. A* **372** (2008) 5872
P. Wang, H. Yang and X. Zhang, *JHEP* **08** (2010) 043
D. Mania and M. Maziashvili, *Phys. Lett. B* **705** (2011) 521
P. Wang, H. Yang and X. Zhang, *Phys. Lett. B* **718** (2012) 265
B. Vakili and M. A. Gorji, *J. Stat. Mech.* (2012) P10013.
- [13] G. Chacón-Acosta, E. Manrique, L. Dagdug and H. A. Morales-Técotl, *SIGMA* **7** (2011) 110.
- [14] G. M. Hossain, V. Husain and S. S. Seahra, *Class. Quantum Grav.* **27** (2010) 165013
E. Castellanos and G. Chacón-Acosta, *Phys. Lett. B* **722** (2013) 119
M. A. Gorji, K. Nozari and B. Vakili, *Phys. Lett. B* **735** (2014) 62.
- [15] S. Das, S. Ghosh and D. Roychowdhury, *Phys. Rev. D* **80** (2009) 125036
S. Das and D. Roychowdhury, *Phys. Rev. D* **81** (2010) 085039
X. Zhang, L. Shao and B.-Q. Ma, *Astropart. Phys.* **34** (2011) 840
N. Chandra and S. Chatterjee, *Phys. Rev. D* **85** (2012) 045012.
- [16] G. M. Hossain, V. Husain and S. Seahra, *Phys. Rev. D* **82** (2010) 124032.
- [17] In momentum polarization, it becomes the Bohr compactification of the real line \mathbb{R}_B [8] that leads to the compact topology for the momentum part of the corresponding phase space (see also [19]).
- [18] V.I. Arnold, *Mathematical Methods of Classical Mechanics* (Springer-Verlag, New York, 1989).
- [19] K. Nozari, M. A. Gorji, V. Hosseinzadeh and B. Vakili, arXiv: 1405.4083 [gr-qc].
- [20] M. A. Gorji, K. Nozari and B. Vakili, *Phys. Rev. D* **89** (2014) 084072.
- [21] M. Chaichian, M. M. Sheikh-Jabbari and A. Tureanu, *Phys. Rev. Lett.* **86** (2001) 2716
S. Das and E. C. Vagenas, *Phys. Rev. Lett.* **101** (2008) 221301
P. Pedram, K. Nozari and S. H. Taheri, *JHEP* **1103** (2011) 093
S. Jalalzadeh, M. A. Gorji and K. Nozari, *Gen. Relativ. Gravit.* **46** (2014) 1632
S. Ghosh, *Class. Quantum Grav.* **31** (2014) 025025.
- [22] A. F. Ali, S. Das and E. C. Vagenas, *Phys. Lett. B* **678** (2009) 497
S. Das, E. C. Vagenas and A. F. Ali, *Phys. Lett. B* **690** (2010) 407.
- [23] We work in unit $k_B = 1 = c$, where k_B and c are the Boltzman constant and speed of light in vacuum respectively.
- [24] R. K. Pathria and P. D. Beale, *Statistical Mechanics* (Elsevier Ltd, Oxford, 2011)
J. Naudts, *Generalised Thermostatistics* (Springer-Verlag, London, 2011).
- [25] Here it is important to note that the correction term is also closely related to the free numerical parameter α which we have set to be of order of unity. In fact the numerical factor α determines the fundamental length scale of the quantum gravity (or lattice discreteness length) as $l_{\text{poly}} = \alpha l_{\text{Pl}}$. Preserving this parameter, one can find an upper bound for the the polymer length scale l_{poly} (see for instance [26]).
- [26] G. Chacón-Acosta and H. Hernandez-Hernandez, arXiv: 1408.1306 [astro-ph.SR]